


Key Fabrications of Chitosan Nanoparticles for Effective Drug Delivery Using Flow Chemistry Reactors

Kampanart Huanbutta¹, Pornsak Sriamornsak^{2,3}, Kittipat Suwanpitak⁴, Nattapat Klinchuen⁴, Thanapat Deebukum⁴, Vasanchai Teppitak⁴, Tanikan Sangnim⁴ 

¹Department of Manufacturing Pharmacy, College of Pharmacy, Rangsit University, Pathum Thani, 12000, Thailand; ²Department of Industrial Pharmacy, Faculty of Pharmacy, Silpakorn University, Nakhon Pathom, 73000, Thailand; ³Academy of Science, the Royal Society of Thailand, Bangkok, 10300, Thailand; ⁴Department of Pharmaceutical Technology, Faculty of Pharmaceutical Sciences, Burapha University, Chonburi, 20131, Thailand

Correspondence: Tanikan Sangnim, Department of Pharmaceutical Technology, Faculty of Pharmaceutical Sciences, Burapha University, Chonburi, 20131, Thailand, Email tanikan@go.buu.ac.th

Introduction: Chitosan nanoparticles have garnered considerable interest in the field of drug delivery owing to their distinctive properties, including biocompatibility, biodegradability, low toxicity, and ability to encapsulate a wide range of drugs. However, the conventional methods (eg, the drop method) for synthesizing chitosan nanoparticles often face limitations in regard to controlling the particle size, morphology, and scalability, hindering their extensive application in drug delivery systems. To overcome these challenges, this study explores using a novel flow chemistry reactor design for fabricating clindamycin-loaded chitosan nanoparticles.

Methods: By varying two critical operating parameters of flow chemistry, namely, the flow rate ratio and total flow rate, the impact of these parameters on the properties of chitosan nanoparticles is investigated using a central composite experimental design.

Results: The optimized conditions for nanoparticle preparation yielded remarkable results, with chitosan nanoparticles exhibiting a small size of 371.60 nm and an extremely low polydispersity index of 0.042. Furthermore, using novel design flow chemistry reactor, the productivity of chitosan nanoparticles was estimated to be 25,402.17 mg/min, which was ~12.71 times higher than that obtained via batch synthesis.

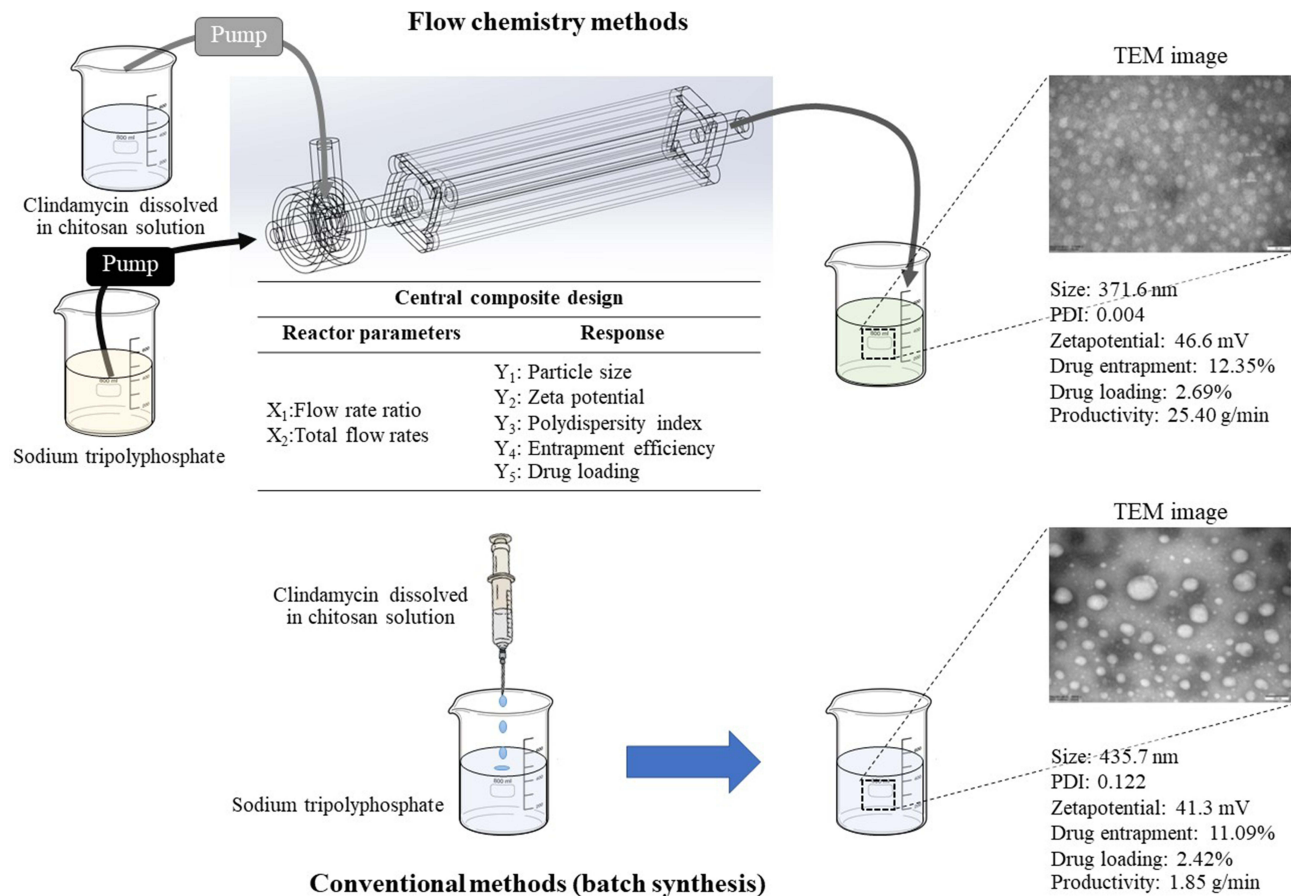
Conclusion: The findings of this study indicate that the use of novel design flow chemistry reactor is promising for synthesizing clindamycin-loaded chitosan nanoparticles and other polymeric nanoparticles intended for drug delivery applications. This is primarily attributed to their ability to produce nanoparticles with a considerably reduced particle size distribution and smaller overall size. The demonstrated high productivity of this technique suggests the potential for industrial-scale nanoparticle manufacturing.

Keywords: chitosan nanoparticles, drug delivery, flow chemistry, sodium tripolyphosphate, continuous manufacturing

Introduction

Nanoparticles for drug delivery have witnessed significant advancements aimed at improving therapeutic outcomes and patient experiences.¹ Among the various nanoparticle drug delivery systems, chitosan nanoparticles have been developed and explored for a decade due to their unique properties, including biocompatibility,² biodegradability,³ reduced toxicity,⁴ easy preparation,² and ability to encapsulate a wide range of drugs.⁵ Chitosan is a natural biopolymer that can be easily functionalized to obtain the desired targeted results and is also approved by Generally Recognized as Safe (GRAS) and the US Food and Drug Administration (US FDA).^{6–10} Moreover, the addition of chitosan can improve the solubility,¹¹ bioavailability,¹² and mucoadhesive properties¹³ of drug delivery systems. Chitosan nanoparticles have been applied in various drug delivery systems, such as colonic drug delivery,⁴ nucleic acid drug delivery,¹⁴ ocular drug delivery,¹⁵ per-oral delivery,^{16–20} pulmonary drug delivery,²¹ nasal drug delivery,²² mucosal drug delivery,²³ gene delivery,²⁴ vaccine delivery and²⁵ vaginal drug delivery,²⁶ as well as for cancer therapy.²⁷ Despite their many advantages and practical uses, chitosan nanoparticles for drug delivery still face certain obstacles, such as their insoluble nature in neutral and alkaline

Graphical Abstract



pH solutions, which restricts their application to environments such as the bloodstream.^{4,6,8} Moreover, the conventional method (ie, dropping drug and chitosan solution on stirred sodium tripolyphosphate (STPP)) used to prepare chitosan nanoparticles often suffers from limitations regarding control over particle size, morphology, and scalability.^{4,5,28} These limitations have hindered their widespread application in drug delivery systems.

To address these challenges, there is a growing interest in developing advanced flow chemistry reactor designs for the rapid and scalable preparation of nanoparticles. Flow chemistry reactors offer several advantages over traditional batch reactors, including precise control over reaction parameters, enhanced reproducibility, and scalability for industrial manufacturing.^{29,30} By leveraging the continuous flow nature of these reactors, efficient mixing and rapid reaction kinetics can be achieved, resulting in improved control over particle properties.³¹ Several nanoparticles for drug delivery, such as PLGA-PEG nanoparticles,³² PLGA-Eudragit nanoparticles,³³ and liposomes,³⁴ have been produced using the flow chemistry method with a microfluidic equipment. However, the production rate per microfluidic reactor is still insufficient for large-scale industries. Moreover, particle formation can easily obstruct small channels in microfluidics reactors.³⁵ Therefore, the advanced design of the mixer and reactor with a high production rate and mixing efficiency in a short time is necessary for the future development of flow chemistry to synthesize nanoparticles.

The objective of this study is to explore the use of new flow chemistry reactor designs for the efficient and scalable synthesis of chitosan nanoparticles in drug delivery systems. Clindamycin HCl as a model drug was selected to investigate the efficacy of nanoparticle production within a novel reactor design intended for the delivery of hydrophilic drugs. Then, the reactor process parameters, including the total flow rates and flow rate ratios between two reactants

(chitosan solution and STPP solution with the model drug), were optimized to achieve the smallest particle size, high drug-loading efficiency, and low particle size distribution, all of which can enhance the application and therapeutic efficiency of chitosan nanoparticles. The chitosan nanoparticles prepared from the novel reactor and batch synthesis in terms of key nanoparticle parameters and production rate were compared. Partial least squares (PLS) models revealing process parameters and particle properties were generated for future chitosan nanoparticle development.

Materials and Methods

Materials

Chitosan (batch no. L112-200330/01) with a molecular weight of 30–80 kDa was acquired from BIO21, Thailand. STPP with a batch number of 221,008 was obtained from Krungthep Chemical, Thailand. Clindamycin HCl was generously provided by Bangkok Lab & Cosmetic Co., Ltd., Thailand. All remaining chemicals used in this study were of pharmaceutical or cosmetic grade.

Fabrications of Chitosan Nanoparticles Using Flow Chemistry

Chitosan nanoparticles were prepared using the ionic gelation method, which is a common method for fabricating chitosan nanoparticles due to its simplicity and effectiveness.^{36–38} In this study, chitosan nanoparticles were prepared using the flow chemistry reactor that was devised and three-dimensionally printed, as described in the previous study.³⁹ The operating mechanism of the reactor involved feeding two liquids into the reactor and allowing them to mix rapidly and uniformly inside the reactor, as shown in Figure 1. For this investigation, two solutions (chitosan with drug and STPP) were combined in the reactor. To prepare the solution input for channel A, chitosan (0.5% w/v) was dispersed in a 1% (v/v) acetic acid solution and stirred gently overnight. After adjusting the pH to 5, clindamycin was solubilized in the chitosan solution to achieve 0.1% (w/v). For the solution input of channel B, 0.05% (w/v) STPP was prepared. Two different solutions were fed to the reactor at varying ratios and total flow rates. Furthermore, the nanoparticles disseminated in the mixture were collected for further analysis.

For comparison, chitosan nanoparticles were prepared using the beaker method, a conventional batch preparation procedure adapted from a previous study by Seila et al.⁴⁰ Chitosan solution with clindamycin at a similar drug-polymer concentration was dropped into STPP aqueous solution (0.05% (w/v)) using the flow chemistry method.

Experimental Design

Herein, experiments were conducted using a central composite design to disclose the effects of the flow chemistry operating parameters and determine the optimal condition. Two factors, ie, the flow rate ratio between channel A and

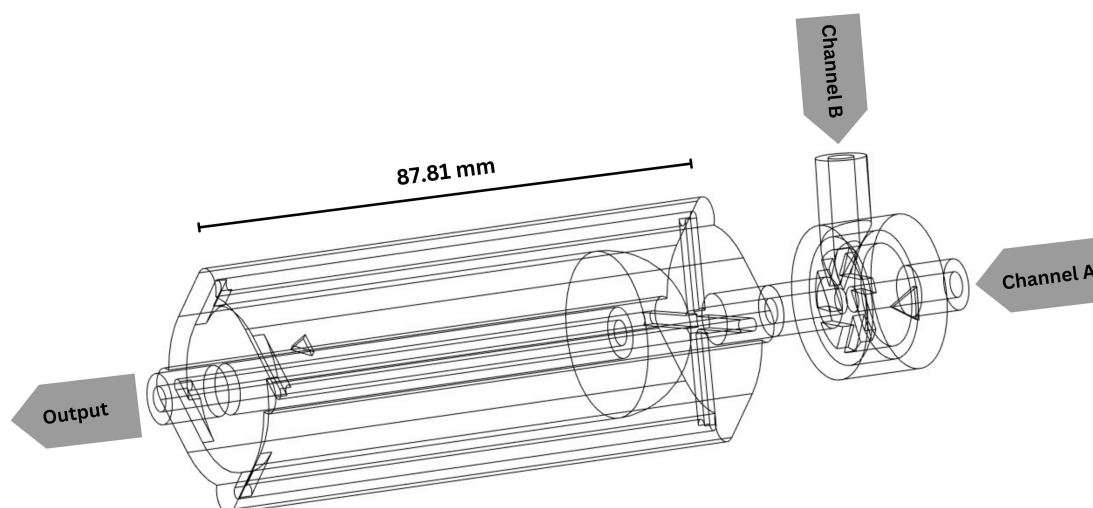


Figure 1 Schematic of reactant flow through the flow chemistry reactor.

Table 1 The Experimental Runs of a 2-Factor, 3-Level Central Composite Design Involved Applying Different Flow Rate Ratios and Total Flow Rates

Run Number	Flow Rate Ratio (X_1)		Total Flow Rate (X_2)	
	Code Value	Actual Value	Code Value	Actual Value (mL/min)
1	-1	3	-1	30
2	1	5	-1	30
3	-1	3	1	100
4	1	5	1	100
5	$-\alpha$	2.59	0	65
6	α	5.41	0	65
7	0	4	$-\alpha$	15.5
8	0	4	α	114.5
9	0	4	0	65
10	0	4	0	65
11	0	4	0	65

channel B (X_1) and the total flow rate (X_2), varied as shown in Table 1. Eleven experimental runs, which contained three central points, were generated using Design-Expert version 10. After the chitosan nanoparticles were prepared according to the experimental design, five responses were accessed, including hydrodynamic diameter (nm, Y_1), zeta potential (mV, Y_2), polydispersity index (Y_3), entrapment efficiency (%), (Y_4), and drug loading (%), (Y_5).

Evaluation of Chitosan Nanoparticle

Hydrodynamic Diameter, Polydispersity Index, and Zeta Potential

The mean diameter, polydispersity index (PDI), and zeta potential of the chitosan nanoparticles were determined using a Zetasizer (MAL1070387, Malvern, UK) to determine their mean diameter, PDI, and zeta potential. Before the analyses, the samples were diluted to 0.5% w/v using deionized water as the solvent and then agitated for 3 min before measurement.⁴¹ The average and standard deviation of the measurements for three batches of samples were reported.

Drug Entrapment Efficiency and Drug Loading

The entrapment efficiency percentage (%EE) of clindamycin in the nanoparticles was determined by separating the free drug from the dispersion of the nanoparticles. The method was modified by referring to a previous study.⁴⁰ Thus, 12 mL of each sample was centrifuged for 30 min at 5000 rpm and 4°C using an ultracentrifugal filter unit (Amicon® Ultra-15 Centrifugal Filter Unit, Merck). The filtrate was then collected and analyzed for clindamycin content through high-performance liquid chromatography using Shimadzu LC-20AD (SPD-M20A, Shimadzu, Nakagyo, Japan). A reverse-phase C18 column 25 cm × 4.6 mm, 5 μm (Phenomenex, USA) was used as the stationary phase, which was maintained at 40°C. As the mobile phase, a mixture of acetonitrile and pH 7.5 phosphate buffer at a ratio of 9:11 (v/v) was used, which flowed isocratically at a rate of 1.0 mL/min. Ultraviolet detection was accessed at 210 nm (SPD-M20A model), and the injection volume of the samples was 10 μL. Then, the %EE was calculated using Eq. (1), considering the total concentration of clindamycin (C_t) used to prepare each nanoparticle sample (C_s).

$$\%EE = \frac{C_t - C_s}{C_t} \times 100 \quad (1)$$

The drug-loading percentage (%DL) was calculated using Eq. (2), considering the total concentration of chitosan used (C_1) to prepare the respective nanoparticle sample.

$$\%DL = \frac{C_t - C_s}{C_t - C_s + C_1} \times 100 \quad (2)$$

Morphology of the Nanoparticles

The morphology of the nanoparticles was analyzed by transmission electron microscopy (TEM; Tecnai 20, Philips, Eindhoven, The Netherlands). The samples were diluted at a ratio of 1:200 (v/v). A sample drop was then placed on a carbon-coated copper grid, followed by negative staining with a 1% aqueous solution of phosphotungstic acid after 15 min. The grid was air-dried thoroughly, and the samples were viewed on a TEM.⁴

Nanoparticle Production Capacity of Flow Chemistry and Batch Synthesis

The production capacities of chitosan nanoparticles prepared by flow chemistry and batch synthesis were compared. The dispersion obtained from both methods was collected and dried. The amount of nanoparticles produced (in milligrams) per minute was then calculated to determine the production capacities of each method.³⁹

Statistical Analysis

Analysis of variance and Levene's test for homogeneity of variance using SPSS version 11.5 for Windows (SPSS Inc., USA) were performed. Depending on whether the Levene's test was insignificant or significant, post hoc testing ($p < 0.05$) of the multiple comparisons was performed using either the Scheffé test or the Games–Howell test, respectively.

Results and Discussion

Properties of the Nanoparticles

In this design space, the hydrodynamic diameter of chitosan nanoparticles (Y_1) produced by the novel design flow chemistry reactor ranged between 272.9 and 393.7 nm. The effect of flow rate ratio (X_1) and total flow rate (X_2) is expressed using the PLS model and response surface, as shown in Table 2 and Figure 2, respectively. As demonstrated in Table 2, the flow rate ratio (between channel A and channel B) and the total flow rate considerably impacted the size of the produced chitosan nanoparticles. The fit of the Y_1 PLS model was statistically considerable, with p values and F values of 0.033 and 17.93, respectively. Figure 2a depicts the response surface of the relation between the hydrodynamic diameter and the ratio of flow rate to total flow rate. As illustrated in the response surface, a high flow rate ratio (high volume of channel A) and a low total flow rate could increase the hydrodynamic diameter. This might be because, during nanoparticle formation, a higher flow rate ratio with a higher volume of channel A (chitosan and drug) and a lower volume of channel B (STPP) lead to a decrease in the mass transfer and reaction rate. This is attributed to a lower cross-linking density, where insufficient cross-linking can result in the formation of larger aggregates instead of well-defined nanoparticles. Additionally, a higher concentration gradient might slow down the cross-linking reaction, allowing more time for particle growth before stabilization occurs.⁴² In addition, a lower total flow rate increases the residence time of the nanoparticles in the reaction or formation zone. Further, longer residence durations may permit increased particle growth or aggregation, resulting in particles with larger sizes.⁴³ The findings of this study align with those of a prior investigation that reported that increased flow rates lead to decreased residence durations, limiting the duration of nucleation and nanoparticle formation.³⁹

Table 2 Partial Least Square (PLS) Regressions Showing the Relationships Between Reactor Operating Conditions and Chitosan Nanoparticle Properties

Response Variables	Unit	PLS Models	P-value	F-Value	R ²
Y_1 Particle size	nm	$Y_1 = 21.54X_1 - 37.6X_2 - 28.25X_1^2 + 368.47$	0.0033*	17.93	0.9472
Y_2 Zeta potential	mV	$Y_2 = 2.09X_2 + 2.10X_1X_2 - 5.09X_1^2X_2 + 4.78X_1X_2^2 + 40.57$	0.0144*	21.51	0.9805
Y_3 Polydispersity index	-	$Y_3 = 0.0207X_1X_2 - 0.0340X_1^2 - 0.463X_2^2 + 0.1012$	0.0034*	17.67	0.9464
Y_4 Entrapment efficiency	%	$Y_4 = 0.786X_2 + 0.3275X_1X_2 + 0.7294X_2^2 - 1.03X_1^2X_2 - 0.5644X_1X_2^2 + 10.52$	0.0112*	25.64	0.9836
Y_5 Drug loading	%	$Y_5 = 0.1671X_2 + 0.0697X_1X_2 + 0.1552X_2^2 - 0.2182X_1^2X_2 - 0.1202X_1X_2^2 + 2.30$	0.0112*	25.62	0.9835

Notes: *Model statistically significant (P value ≤ 0.05).

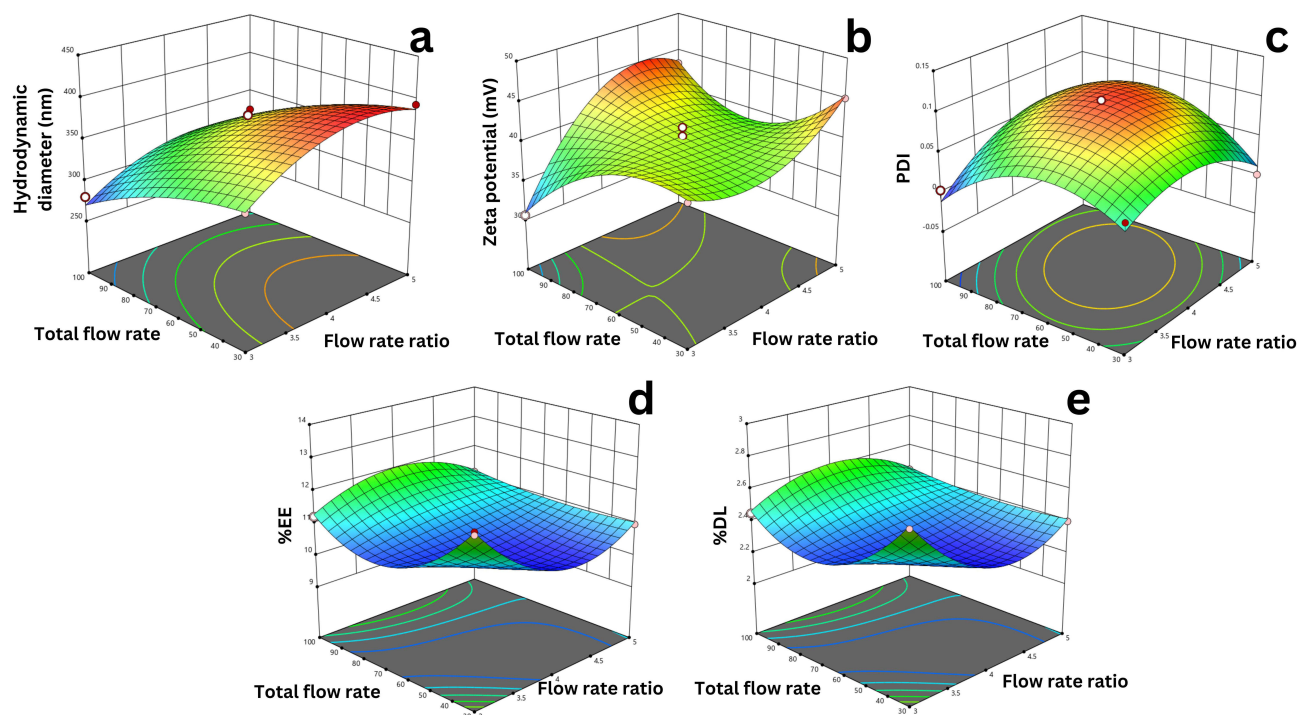


Figure 2 Response surface plots (three-dimensional) showing the influences of different flow rate ratios and total flow rates on (a) particle size, (b) zeta potential, (c) polydispersity index, (d) entrapment efficiency, and (e) drug loading.

In all the experimental runs, the zeta potential values (Y_2) of the chitosan nanoparticles were between 30.6 and 45.6 mV. Chitosan nanoparticles often exhibit positive zeta potential values due to the presence of amino groups ($-\text{NH}_2$) on the chitosan polymer chain. The positive zeta potential arises from the protonation of the amino groups in an aqueous environment.⁴ The positive zeta potential of chitosan nanoparticles, which is >30 mV, generates electrostatic repulsion between particles with similar charges. This repulsion prevents nanoparticles from aggregating or adhering to one another, stabilizing the suspension and preserving particle dispersion.⁴⁴

According to Table 2, the total flow rate (X_2) and the interaction between the flow rate ratio (X_1) and the total flow rate (X_2) have considerable effects on the zeta potential values of chitosan nanoparticles. As illustrated in Figure 2b, the relation between them is quadratic (a curved or nonlinear relation). Changes in the concentration of chitosan can influence the charge density of the nanoparticles. At low and high concentrations, the charge density may vary with changes in the flow rate ratio and total flow rate. Moreover, the interaction between these factors can lead to complex particle growth and aggregation behaviors. Depending on the specific conditions, there may be an optimal range of flow rate ratio and total flow rate, in which the zeta potential values are maximized or minimized, resulting in a quadratic relation.⁴⁵

The PDI values of chitosan nanoparticles (Y_3) prepared from the novel design flow chemistry reactor were surprisingly low, ranging between 0.001 and 0.106, which indicates a high level of size uniformity. As presented in Table 2, PLS regression conducted to predict PDI values (Y_3) was considerably fit at a p value of 0.0034 and an F value of 17.67. Figure 2c presents the response surface illustrating the impact of the total flow rate and flow rate ratio on PDI. It reveals that PDI rose when the experimental run was in the middle of the design space. Therefore, the perimeter of the design space offered an exceptionally low PDI, according to the response surface plot. This may be because a total flow rate that is too low or too high and not a proper chitosan and STPP mixing ratio resulted in inconsistent particle formation in the reactor, as reported previously.³⁹

According to Table 2, The %EE of the chitosan nanoparticles (Y_4) under the experimental design was between 10.36% and 13.16%. The PLS regression of %EE (Y_4) was considerably fit at a p value of 0.0112 and an F value of 25.64. As shown in Figure 2d, their relation was quadratic. However, the resulting %EE was not high, despite the

significant effects of the total flow rate (X_2) and the interaction between the flow rate ratio (X_1) and the total flow rate (X_2) on %EE. The observed low %EE can be attributed to the high solubility of the model drug (clindamycin HCl) in water, which may result in drug leakage during particle formation⁴⁶ as well as short retention time in the reactor and mixer. The fast dissolution of the drug hinders its effective encapsulation, particularly for hydrophilic drugs, which require more time for entrapment.⁴⁷ Furthermore, it has been previously observed that the high mixing index of the vortex reactor can effectively improve drug solubility during the particle production process. This factor contributes to the diminished efficacy of nanoparticle drug entrapment.³⁹ However, in future studies, optimizing formulation parameters and process conditions, such as adjusting the drug-to-polymer ratio and adding more mixer connections to extend the retention time, may help enhance drug entrapment efficiency.

In all experimental runs, the %DL (Y_5) was in the range of 2.36%–2.86%. The results obtained from the PLS model, as presented in Table 2 and Figure 2e, indicate that the total flow rate (X_2) and interaction between the flow rate ratio (X_1) and the total flow rate (X_2) exhibited a significant effect on %DL ($p = 0.0112$). However, the observed %DL was not considerably high, similar to the previously discussed low %EE. This suggests that the factors contributing to the limited drug loading are likely analogous to those affecting the drug entrapment process, as previously described. Further investigations and optimization strategies are warranted to improve drug loading in future endeavors.

Optimization and Predictability of the PLS Model

Valuable insights into the optimization of conditions for preparing desired chitosan nanoparticles were obtained from the PLS regression models and response surfaces. Based on the determined constraints and desirability of the responses (Table 3), the optimized conditions were X_1 (flow rate ratio) = 3 and X_2 (total flow rate) = 30 mL/min, resulting in a desirability value of 0.652. Further, the predicted responses from the PLS regression models were compared with the actual test values and the prediction ability percentages were calculated, as shown in Table 4. The analysis revealed that the PLS regression models exhibited a considerable degree of predictive capability across all responses, with accuracy levels ranging from 67.39% to 99.94%. Three responses, namely, Y_2 (zeta potential), Y_4 (entrapment efficiency), and Y_5 (drug loading), demonstrated excellent predictive capability. These findings indicated that the regression models

Table 3 Constraint and Desirability of Independent Variable (X) and Responses (Y)

Independent variable (X)		Constraint	Request to
X_1	Flow rate ratio	$2.59 \leq X_1 \leq 5.41$	In range
X_2	Total flow rates (mL/min)	$15.5 \leq X_2 \leq 114.5$	In range
Responses (Y)		Predicting range	Target to
Y_1	Particle size (nm)	$272.9 \leq Y_1 \leq 393.7$	Minimize
Y_2	Zeta potential (mV)	$30.6 \leq Y_2 \leq 45.6$	Maximize
Y_3	Polydispersity index	$0.001 \leq Y_3 \leq 0.106$	Minimize
Y_4	Entrapment efficiency (%)	$10.36 \leq Y_4 \leq 13.16$	Maximize
Y_5	Drug loading (%)	$2.36 \leq Y_5 \leq 2.86$	Maximize

Table 4 Comparison Between the Predicted Responses from the Partial Least Squares Regression Models, Actual Test Values, and Prediction Ability Percentages

Responses	Predicted Responses	Actual Test Values	Prediction Ability Percentages
Y_1	341.14 nm	371.60 nm	91.08%
Y_2	41.07 mV	41.10%	99.94%
Y_3	0.032	0.042	67.39%
Y_4	12.42%	12.35%	99.45%
Y_5	2.70%	2.69%	99.45%

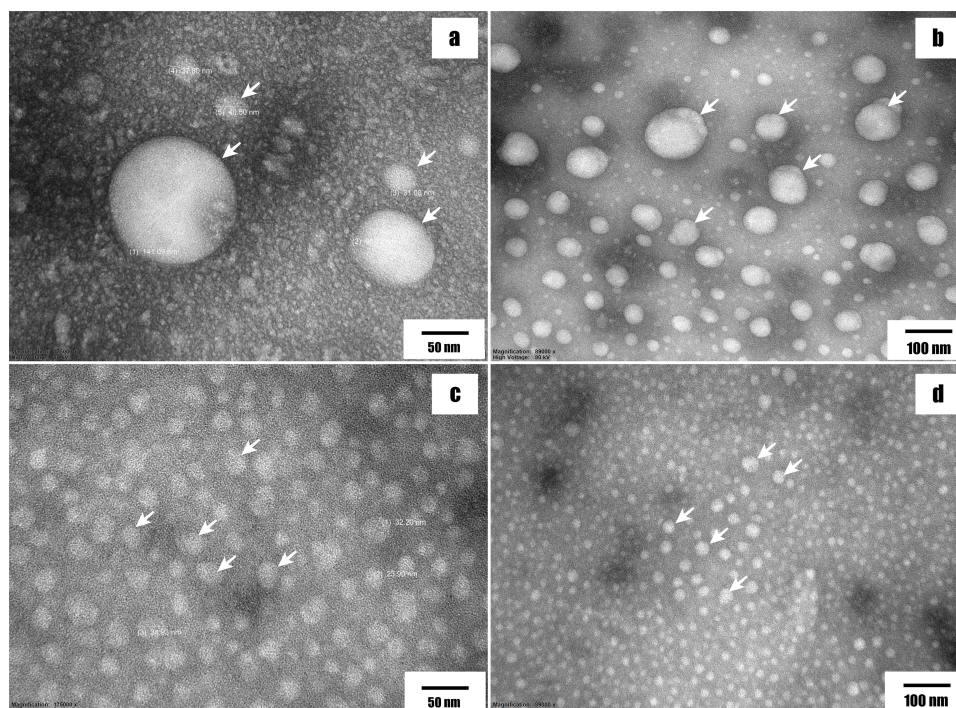


Figure 3 Transmission electron microscopic images of chitosan nanoparticles synthesized using (a and b) the novel design flow chemistry reactor and (c and d) the batch synthesis method (white arrows indicate chitosan nanoparticles).

successfully captured the relation between the operating parameters and their specific responses. The accurate predictions of the operating parameters further validated the effectiveness of the PLS regression models in understanding and optimizing the synthesis of chitosan nanoparticles.

Particle Morphology

The particle morphology of the chitosan nanoparticles synthesized using batch synthesis and the novel design flow chemistry reactor were examined through TEM, as illustrated in Figures 3a-d, respectively. Both techniques provided spherical-shaped particles. The chitosan nanoparticles produced using batch synthesis exhibited an average size ranging from 30 to 120 nm. This value was considerably greater than that of the nanoparticles produced using the novel design flow chemistry reactor, which had a diameter of ~40–60 nm. This observation aligns with the size report obtained using the dynamic light scattering technique (Y_1). The particle size determined via TEM was smaller than that determined via dynamic light scattering methodology (hydrodynamic diameter). TEM is less likely to be affected by factors such as the shape of the particles or the presence of aggregates. Moreover, TEM has a higher resolution than light scattering. This implies that TEM has the capability of discerning finer details within the structure of particles.^{48,49}

Furthermore, as compared with the nanoparticles produced using the novel design flow chemistry reactor, the size dispersion of the chitosan nanoparticles obtained from batch synthesis exhibited noticeable variations. The disparities in particle morphology, size, and size dispersion among the chitosan nanoparticles synthesized through batch synthesis and the novel design flow chemistry reactor can be attributed to several factors. Using the batch synthesis method, which involves a bulk preparation process, may result in slower and less controlled mixing, leading to an uneven distribution of reactants and subsequent particle formation, resulting in a wider size dispersion. On the contrary, the continuous flow nature of the flow chemistry design enables precise control over reaction parameters and improved mixing efficiency, resulting in better homogeneous nucleation and particle growth. This promotes a narrower size distribution and a smaller average particle size.^{50,51}

Table 5 Comparative Information Regarding Chitosan Nanoparticles Prepared Using Batch Synthesis (Conventional Method) and the Novel Design Flow Chemistry

Nanoparticle Properties	Preparation Method		P-value
	Batch Synthesis	Flow Chemistry	
Particle size	435.73±52.71 nm	371.60±83.92 nm	0.046*
Zeta potential	41.30±1.22 mV	41.07±0.72 mV	0.439
Polydispersity index	0.12±0.00	0.04±0.00	<0.001**
Entrapment efficiency	11.10±0.02%	12.35±0.04%	<0.001**
Drug loading	2.43±0.00%	2.69±0.01%	<0.001**
Productivity	1,852.05±8.76 mg/min	25,402.50±79.35 mg/min	<0.001**

Notes: *p-value < 0.05, ** p-value < 0.001.

Nanoparticle Production Capacity of Flow Chemistry and Batch Synthesis

Table 5 presents comparative information regarding chitosan nanoparticles prepared using batch synthesis (the conventional method) and the novel design flow chemistry reactor. Moreover, the table provides a comprehensive overview of the properties, including size, zeta potential, polydispersity index, entrapment efficiency, and drug loading, as well as the manufacturing productivity of chitosan nanoparticles synthesized through batch synthesis and the novel design flow chemistry reactor. The hydrodynamic diameter and polydispersity index of the chitosan nanoparticles synthesized through flow chemistry were considerably lower than those obtained through batch synthesis. The disparities we observed in the properties and manufacturing productivity of chitosan nanoparticles synthesized through batch synthesis and the innovative design of flow chemistry were consistent with the findings obtained from the TEM morphology analysis, as presented in the results and discussion of particle morphology. In addition, the productivity of chitosan nanoparticles achieved through flow chemistry was considerably higher, ~12.71 times greater, than that of the batch synthesis method. These findings emphasize the advantages of recent design flow chemistry in terms of enhanced control, uniformity, and scalability for synthesizing chitosan nanoparticles at the industrial production level.

Compared with the study of microfluidic flow chemistry by Fatemeh et al⁵² the present investigation demonstrated that the size of the chitosan nanoparticles obtained through the novel flow chemistry design was larger, ranging between 272.9 and 393.7 nm. This disparity in size can be attributed to the longer residence time in the flow chemistry system, which allows for increased particle growth.⁵³ However, the PDI of the nanoparticles synthesized through flow chemistry was considerably lower than the microfluidic approach. This indicates a higher level of size uniformity and a more homogeneous distribution of particles in the flow chemistry system. In addition, a notable advantage of the contemporary flow chemistry design is its considerably higher productivity compared to microfluidic technology, allowing for a faster and more efficient synthesis of chitosan nanoparticles.

Conclusions

The use of advanced flow chemistry reactor designs to synthesize chitosan nanoparticles in drug delivery systems holds great promise for improving nanoparticle production efficiency and their properties. This study successfully optimized the parameters of the reactor process, including flow rate ratios and total flow rates, to achieve the desired nanoparticle properties. The PLS regression models obtained from the CCD experimental design exhibited satisfactory predictability, providing valuable insights regarding the relation between the reactor operating conditions and nanoparticle properties. The use of novel design flow chemistry reactor resulted in the production of drug-loaded chitosan nanoparticles exhibiting notably reduced particle sizes and an exceptionally low polydispersity. Furthermore, the nanoparticle synthesis productivity obtained through flow chemistry was considerably greater than that obtained via batch synthesis. Nevertheless, when loading highly soluble drugs into nanoparticles, it is imperative to continuously monitor the drug-loading percentage and drug encapsulation effectiveness. The observed occurrence can be attributed to the notable efficacy in mixing and the short period of material retention within the vortex reactor. Overall, this study underscores the potential of the advanced flow chemistry reactor design as an efficient and scalable approach for synthesizing chitosan

nanoparticles or other polymeric nanoparticles, contributing to advancements in drug delivery systems and enhancing the therapeutic efficacy. To substantiate the efficacy of this novel mixer and reactor design in the manufacture of drug delivery nanoparticles, additional investigations including different model drugs and alternative nanoparticle formations, such as liposomes, ethosomes, solid lipid nanoparticles, and others, are necessary.

Abbreviations

US FDA, United States Food and Drug Administration; STPP, Sodium tripolyphosphate; PDI, Polydispersity index; HPLC, High-performance liquid chromatography; FRT, Flow rate ratio; TFR, Total flow rate; PLS, Partial least squares; %EE, Percentage of entrapment efficiency; %DL, Percentage of drug loading; TEM, Transmission electron microscopy.

Acknowledgments

The authors express their gratitude to the Faculty of Pharmaceutical Sciences, Burapha University for generously providing laboratory equipment and financial support. Additionally, the authors would like to acknowledge and appreciate the support received from the College of Pharmacy, Rangsit University and the Faculty of Pharmacy, Silpakorn University.

Author Contributions

All authors made a significant contribution to the work reported, whether that is in the conception, study design, execution, acquisition of data, analysis and interpretation, or in all these areas; took part in drafting, revising or critically reviewing the article; gave final approval of the version to be published; have agreed on the journal to which the article has been submitted; and agree to be accountable for all aspects of the work.

Disclosure

The authors declare no conflicts of interest.

References

1. Sharma A, Shambhwani D, Pandey S, et al. Advances in lung cancer treatment using nanomedicines. *ACS omega*. 2022;8(1):10–41. doi:10.1021/acsomega.2c04078
2. Yanat M, Schroën K. Preparation methods and applications of chitosan nanoparticles; with an outlook toward reinforcement of biodegradable packaging. *React Funct Polym*. 2021;161:104849. doi:10.1016/j.reactfunctpolym.2021.104849
3. El-Naggar NE-A, Shiha AM, Mahrous H, Mohammed AA. Green synthesis of chitosan nanoparticles, optimization, characterization and antibacterial efficacy against multi drug resistant biofilm-forming *Acinetobacter baumannii*. *Sci Rep*. 2022;12(1):19869. doi:10.1038/s41598-022-24303-5
4. Huanbutta K, Sriamornsak P, Luangtana-Anan M, et al. Application of multiple stepwise spinning disk processing for the synthesis of poly (methyl acrylates) coated chitosan–diclofenac sodium nanoparticles for colonic drug delivery. *Eur. J. Pharm. Sci*. 2013;50(3–4):303–311. doi:10.1016/j.ejps.2013.07.010
5. Huanbutta K, Terada K, Sriamornsak P, Nunthanid J. Simultaneous X-ray diffraction-differential scanning calorimetry and physicochemical characterizations of spray dried drugs and chitosan microspheres. *Walailak J Sci Technol*. 2016;13(10):849–861.
6. Kaur M, Sharma A, Puri V, et al. Chitosan-Based Polymer Blends for Drug Delivery Systems. *Polymers*. 2023;15(9):2028. doi:10.3390/polym15092028
7. Sangnim T, Sriamornsak P, Singh I, Huanbutta K. Swallowing Gel for Patients with Dysphagia: a Novel Application of Chitosan. *Gels*. 2021;7(3):108. doi:10.3390/gels7030108
8. Huanbutta K, Sangnim T, Cheewatanakornkool K, Sutthapitaksakul L, Thanawuth K, Sriamornsak P. Physical stability of different chitosan salts in matrix tablet formulations. *Pharm Sci Asia*. 2020;47(4):347–356. doi:10.29090/psa.2020.04.019.0098
9. Huanbutta K, Sriamornsak P, Limmatvapirat S, et al. Swelling kinetics of spray-dried chitosan acetate assessed by magnetic resonance imaging and their relation to drug release kinetics of chitosan matrix tablets. *Eur. J. Pharm. Biopharm*. 2011;77(2):320–326. doi:10.1016/j.ejpb.2010.11.019
10. Huq T, Khan A, Brown D, Dhayagude N, He Z, Ni Y. Sources, production and commercial applications of fungal chitosan: a review. *J Bioresources Bioprod*. 2022;7(2):85–98. doi:10.1016/j.jobab.2022.01.002
11. Obeidat WM, Gharaibeh SF, Jaradat A. The Influence of Drugs Solubilities and Chitosan-TPP Formulation Parameters on the Mean Hydrodynamic Diameters and Drugs Entrapment Efficiencies into Chitosan-TPP Nanoparticles. *AAPS Pharm Sci Tech*. 2022;23(7):262. doi:10.1208/s12249-022-02420-8
12. Thanou M, Verhoef J, Junginger H. Oral drug absorption enhancement by chitosan and its derivatives. *Adv. Drug Delivery Rev*. 2001;52(2):117–126. doi:10.1016/S0169-409X(01)00231-9
13. Amin MK, Boateng JS. Enhancing stability and mucoadhesive properties of chitosan nanoparticles by surface modification with sodium alginate and polyethylene glycol for potential oral mucosa vaccine delivery. *Mar Drugs*. 2022;20(3):156. doi:10.3390/md20030156

14. Jaferník K, Ladniak A, Blicharska E, et al. Chitosan-Based Nanoparticles as Effective Drug Delivery Systems—A review. *Molecules*. 2023;28(4):1963. doi:10.3390/molecules28041963
15. Pal K, Pradhan BK, Kim D, Jarzębski M. Chitosan-based nanoparticles for ocular drug delivery. *Adv Biomed Polymers Composites Elsevier*. 2023;247–263.
16. Choukaifé H, Seyam S, Alallam B, Doolaanea AA, Alfatama M. Current Advances in Chitosan Nanoparticles Based Oral Drug Delivery for Colorectal Cancer Treatment. *Int J Nanomed*. 2022;3933–3966. doi:10.2147/IJN.S375229
17. Sangnim T, Dheer D, Jangra N, Huanbutta K, Puri V, Sharma A. Chitosan in Oral Drug Delivery Formulations: a Review. *Pharmaceutics*. 2023;15(9):2361. doi:10.3390/pharmaceutics15092361
18. Huanbutta K, Cheewatanakornkool K, Terada K, Nunthanid J, Sriamornsak P. Impact of salt form and molecular weight of chitosan on swelling and drug release from chitosan matrix tablets. *Carbohydr. Polym*. 2013;97(1):26–33. doi:10.1016/j.carbpol.2013.04.073
19. Nunthanid J, Luangtana-Anan M, Sriamornsak P, Limmatvapirat S, Huanbutta K, Puttipipatkachorn S. Use of spray-dried chitosan acetate and ethylcellulose as compression coats for colonic drug delivery: effect of swelling on triggering in vitro drug release. *Eur. J. Pharm. Biopharm*. 2009;71(2):356–361. doi:10.1016/j.ejpb.2008.08.002
20. Huanbutta K, Luangtana-Anan M, Sriamornsak P, Limmatvapirat S, Puttipipatkachorn S, Nunthanid J. Factors affecting preparations of chitosan microcapsules for colonic drug delivery. *J Met Mater Miner*. 2008;18(2):56.
21. Islam N, Dmour I, Taha MO. Degradability of chitosan micro/nanoparticles for pulmonary drug delivery. *Heliyon*. 2019;5(5):e01684. doi:10.1016/j.heliyon.2019.e01684
22. Li J, Cai C, Li J, et al. Chitosan-based nanomaterials for drug delivery. *Molecules*. 2018;23(10):2661. doi:10.3390/molecules23102661
23. Martirosyan A, Olesen MJ, Howard KA. Chitosan-based nanoparticles for mucosal delivery of RNAi therapeutics. *Adv Genet*. 2014;88:325–352.
24. Xue Y, Wang N, Zeng Z, Huang J, Xiang Z, Guan Y-Q. Neuroprotective effect of chitosan nanoparticle gene delivery system grafted with acteoside (ACT) in Parkinson's disease models. *J Mater Sci Technol*. 2020;43:197–207. doi:10.1016/j.jmst.2019.10.013
25. Mehrabi M, Montazeri H, Mohamadpour Dounighi N, Rashti A, Vakil-Ghartavol R. Chitosan-based nanoparticles in mucosal vaccine delivery. *Arch. Razi Inst*. 2018;73(3):165–176. doi:10.22092/ari.2017.109235.1101
26. Tuğcu-Demiröz F, Saar S, Kara AA, Yıldız A, Tunçel E, Acartürk F. Development and characterization of chitosan nanoparticles loaded nanofiber hybrid system for vaginal controlled release of benzydamine. *Eur. J. Pharm. Sci*. 2021;161:105801. doi:10.1016/j.ejps.2021.105801
27. Rostami E. Progresses in targeted drug delivery systems using chitosan nanoparticles in cancer therapy: a mini-review. *J Drug Delivery Sci Technol*. 2020;58:101813. doi:10.1016/j.jddst.2020.101813
28. Khan IU, Serra CA, Anton N, Vandamme TF. Production of nanoparticle drug delivery systems with microfluidics tools. *Expert Opin Drug Delivery*. 2015;12(4):547–562. doi:10.1517/17425247.2015.974547
29. Holtze C, Boehling R. Batch or flow chemistry?—a current industrial opinion on process selection. *Curr. Opin. Chem. Eng*. 2022;36:100798. doi:10.1016/j.coche.2022.100798
30. Długosz O, Banach M. Inorganic nanoparticle synthesis in flow reactors—applications and future directions. *React Chem Eng*. 2020;5(9):1619–1641. doi:10.1039/D0RE00188K
31. Swisher JH, Jibril L, Petrosko SH, Mirkin CA. Nanoreactors for particle synthesis. *Nature Rev Mater*. 2022;7(6):428–448.
32. Xu J. *Synthesis of Polymeric Nanoparticles for the Controlled Release of Hydrophobic and Hydrophilic Therapeutic Compounds*. Université de Bordeaux; 2016.
33. Zoqlam R, Morris CJ, Akbar M, et al. Evaluation of the benefits of microfluidic-assisted preparation of polymeric nanoparticles for DNA delivery. *Mater Sci Eng C*. 2021;127:112243. doi:10.1016/j.msec.2021.112243
34. Kastner E, Verma V, Lowry D, Perrie Y. Microfluidic-controlled manufacture of liposomes for the solubilisation of a poorly water soluble drug. *Int J Pharm*. 2015;485(1–2):122–130. doi:10.1016/j.ijpharm.2015.02.063
35. Elvira KS, I Solvas XC, Wootton RC, Demello AJ. The past, present and potential for microfluidic reactor technology in chemical synthesis. *Nature Chem*. 2013;5(11):905–915. doi:10.1038/nchem.1753
36. Desai KG. Chitosan nanoparticles prepared by ionotropic gelation: an overview of recent advances. *Critical Reviews™ in Therapeutic Drug Carrier Systems*. 2016;33(2):107–158. doi:10.1615/CritRevTherDrugCarrierSyst.2016014850
37. Fan W, Yan W, Xu Z, Ni H. Formation mechanism of monodisperse, low molecular weight chitosan nanoparticles by ionic gelation technique. *Colloids Surf., B*. 2012;90:21–27. doi:10.1016/j.colsurfb.2011.09.042
38. Kunjachan S, Jose S, Lammers T. Understanding the mechanism of ionic gelation for synthesis of chitosan nanoparticles using qualitative techniques. *Asian J Pharmaceutics*. 2010;4(2):56.
39. Suwanpitak K, Sriamornsak P, Singh I, Sangnim T, Huanbutta K. Three-Dimensional-Printed Vortex Tube Reactor for Continuous Flow Synthesis of Polyglycolic Acid Nanoparticles with High Productivity. *Nanomaterials*. 2023;13(19):2679. doi:10.3390/nano13192679
40. Tolentino S, Pereira MN, Cunha-Filho M, Gratieri T, Gelfuso GM. Targeted clindamycin delivery to pilosebaceous units by chitosan or hyaluronic acid nanoparticles for improved topical treatment of acne vulgaris. *Carbohydr. Polym*. 2021;253:117295. doi:10.1016/j.carbpol.2020.117295
41. Huanbutta K, Sangnim T, Limmatvapirat S, Nunthanid J, Sriamornsak P. Design and characterization of prednisolone-loaded nanoparticles fabricated by electrohydrodynamic atomization technique. *Chem. Eng. Res. Des*. 2016;109:816–823. doi:10.1016/j.cherd.2016.03.004
42. Akbari M, Rahimi Z, Rahimi M. Chitosan/tripolyphosphate nanoparticles in active and passive microchannels. *Res Pharm Sci*. 2021;16(1):79. doi:10.4103/1735-5362.305191
43. Ling FW, Abdulbari HA, Sim-Yee C. Effect of residence time on the morphology of silica nanoparticles synthesized in a microfluidic reactor. *J Flow Chem*. 2022;12(1):17–30. doi:10.1007/s41981-021-00175-0
44. Rasmussen MK, Pedersen JN, Marie R. Size and surface charge characterization of nanoparticles with a salt gradient. *Nat Commun*. 2020;11(1):2337. doi:10.1038/s41467-020-15889-3
45. Athavale R, Sapre N, Rale V, et al. Tuning the surface charge properties of chitosan nanoparticles. *Mater Lett*. 2022;308:131114. doi:10.1016/j.matlet.2021.131114
46. Khattab A, Nattouf A. Optimization of entrapment efficiency and release of clindamycin in microsphere based gel. *Sci Rep*. 2021;11(1):23345. doi:10.1038/s41598-021-02826-7
47. Guidi M, Seeberger PH, Gilmore K. How to approach flow chemistry. *Chem. Soc. Rev*. 2020;49(24):8910–8932. doi:10.1039/C9CS00832B
48. Merkus HG. *Particle Size Measurements: Fundamentals, Practice, Quality*. Vol. 17. Springer Science & Business Media; 2009.

49. Brar SK, Verma M. Measurement of nanoparticles by light-scattering techniques. *TrAC Trends in Analytical Chemistry*. 2011;30(1):4–17. doi:10.1016/j.trac.2010.08.008
50. Sreekumar S, Goycoolea FM, Moerschbacher BM, Rivera-Rodriguez GR. Parameters influencing the size of chitosan-TPP nano-and microparticles. *Sci Rep*. 2018;8(1):4695. doi:10.1038/s41598-018-23064-4
51. Luo G, Du L, Wang Y, Lu Y, Xu J. Controllable preparation of particles with microfluidics. *Particuology*. 2011;9(6):545–558. doi:10.1016/j.partic.2011.06.004
52. Majedi FS, Hasani-Sadrabadi MM, Emami SH, et al. Microfluidic synthesis of chitosan-based nanoparticles for fuel cell applications. *Chem. Commun*. 2012;48(62):7744–7746. doi:10.1039/c2cc33253a
53. Liao Y, Mechulam Y, Lassalle-Kaiser B. A millisecond passive micromixer with low flow rate, low sample consumption and easy fabrication. *Sci Rep*. 2021;11(1):20119. doi:10.1038/s41598-021-99471-x

International Journal of Nanomedicine

Dovepress

Publish your work in this journal

The International Journal of Nanomedicine is an international, peer-reviewed journal focusing on the application of nanotechnology in diagnostics, therapeutics, and drug delivery systems throughout the biomedical field. This journal is indexed on PubMed Central, MedLine, CAS, SciSearch®, Current Contents®/Clinical Medicine, Journal Citation Reports/Science Edition, EMBase, Scopus and the Elsevier Bibliographic databases. The manuscript management system is completely online and includes a very quick and fair peer-review system, which is all easy to use. Visit <http://www.dovepress.com/testimonials.php> to read real quotes from published authors.

Submit your manuscript here: <https://www.dovepress.com/international-journal-of-nanomedicine-journal>